A Potential Chemotherapeutic Strategy for the Selective Inhibition of Promutagenic DNA Synthesis by Nonnatural Nucleotides†

Xuemei Zhang,‡ Irene Lee,§ and Anthony J. Berdis*,‡

Departments of Pharmacology and Chemistry, Case Western Reserve University, 10900 Euclid Avenue, Cleveland, Ohio 44106

Received March 30, 2005; Revised Manuscript Received June 27, 2005

ABSTRACT: This manuscript reports the development of nonnatural nucleotide analogues that are preferentially incorporated opposite an abasic site, a common form of DNA damage. Competition experiments confirm that all of the nonnatural nucleotides tested are poorly incorporated into unmodified DNA. However, two analogues that contain extensive π-electron density (5-nitro-indolyl-2′deoxyriboside triphosphate (5-NITP) and 5-phenyl-indolyl-2′deoxyriboside triphosphate (5-PhITP)) are selectively inserted opposite an abasic site and can prevent the incorporation of natural dNTPs. We demonstrate that the DNA polymerase is unable to extend beyond the incorporated nonnatural nucleotide, a result that provides direct evidence for their unique chain termination capabilities. Furthermore, these nonnatural analogues are more slowly excised once inserted opposite the DNA lesion compared to natural dNTPs. The rate of excision becomes significantly faster when the nonnatural analogues are paired opposite natural templating positions, a result that provides additional evidence for their preferential insertion opposite the DNA lesion. Moreover, idle turnover measurements confirm that the bacteriophage T4 polymerase more stably incorporates 5-NIMP and 5-PhIMP opposite damaged DNA compared to natural dNTPs. The reduced idle turnover of these analogues reflects favorable insertion kinetics coupled with reduced exonuclease-proofreading capacity. Collectively, these data demonstrate the ability to selectively inhibit translesion DNA synthesis in vitro. A novel strategy is proposed to potentially use these nucleoside analogues to enhance the chemotherapeutic effects of DNA damaging agents as well as a possible chemopreventive strategy to inhibit promutagenic DNA replication.

DNA replication is absolutely essential for cellular proliferation. As such, chemotherapeutic agents that compromise the integrity of nucleic acid are important components in modern medical efforts to combat hyperproliferative diseases such as cancer (*1*) and autoimmune dysfunctions (*2*), as well as viral (*3*) and microbial (*4*) infections. Compounds such as temozolomide (*5*), cyclophosphamide (*6*), and cisplatin (*7*) are effective chemotherapeutic agents since they significantly modify nucleic acid and inhibit DNA synthesis, DNA repair, or both to prevent cellular proliferation. However, the widespread use of these agents is limited by two major complications. First, they are nonselective DNA damaging agents that target all rapidly proliferating cells and can cause unwanted side effects. Second, these agents induce lesions that can be inappropriately replicated to cause further mutagenesis, an event that could enhance disease development. Indeed, translesion DNA synthesis represents a possible route for the initiation of drug resistance (*8*), genetic variations associated with solid tumors (*9*−*11*), and the development of secondary cancers in response to chemotherapy (*12*−*14*).

These concerns have prompted initiatives to design more selective drugs targeting specific enzymes involved in nucleic acid metabolism. Arguably, the most successful of these agents are nucleotide analogues such as zidovudine (AZT) (*15*) and acyclovir (*16*) that act as chain terminators of DNA synthesis. The use of chain terminators has historically been associated with the treatment of viruses such as HIV (*17*, *18*) and herpes simplex virus (*19*). However, these and other analogues such as araC[1] and fludaribine have also been used to treat various hyperproliferative malignancies such as cancer (*20*). Unfortunately, the therapeutic utility of these nucleotide analogues is often limited by three interrelated complications. The most prevalent of these is the excision of the enzymatically inserted nucleotide from the primer−template to reverse chain termination and allow for the reinitiation of DNA synthesis. Viral polymerases typically use pyrophosphorolysis to remove chain terminators from DNA (*21*), while eukaryotes effectively excise the inserted chain terminator through their associated exonuclease proofreading activity (*22*). Either activity provides a mechanism for drug resistance. Another complication is that these inhibitors contain alterations in the ribose moiety while the

† This research was supported through funding from the American Cancer Society Cuyahoga Unit to A.J.B. (Grant 021203A) and from the Presidential Research Initiative to I.L.

* Corresponding Author. Telephone (216)-368-4723, fax (216) 368-3395, e-mail ajb15@case.edu.

‡ Department of Pharmacology.

§ Department of Chemistry.

[1] Abbreviations: araC, cytosine arabinoside; TBE, Tris-HCl/borate/EDTA; EDTA; ethylenediaminetetraacetate, sodium salt; dNTP, deoxynucleoside triphosphate; 5-NITP, 5-nitro-indolyl-2′deoxyriboside triphosphate; 5-PhITP, 5-phenyl-indolyl-2′-deoxyriboside triphosphate; gp43 exo$^+$, wild-type bacteriophage T4 DNA polymerase; gp43 exo$^-$, an exonuclease-deficient mutant of the bacteriophage T4 DNA polymerase.

10.1021/bi050584n CCC: $30.25
Published on Web 09/03/2005

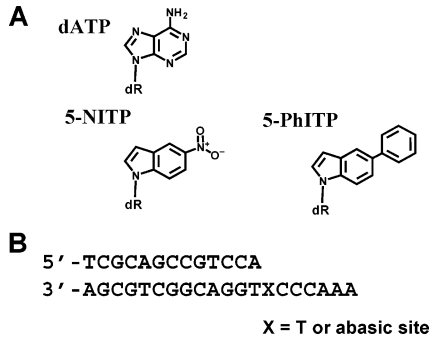

FIGURE 1: (A) Structures of 2′-deoxynucleoside triphosphates used in this study, dATP, 5-NITP, and 5-PhITP. For convenience, dR is used to represent the deoxyribose triphosphate portion of the nucleotide. (B) Defined DNA substrates used for kinetic analysis. "X" in the template strand denotes thymine or the presence of a tetrahydrofuran moiety that functionally mimics an abasic site.

nucleobase portion remains identical to that of a natural nucleoside. With the exception of error prone DNA polymerases such as pol ζ (*23*) and pol ϵ (*24*), all replicative DNA polymerases to date rely heavily if not exclusively on the formation of classic Watson−Crick base pairs during the process of DNA replication. Thus, current chain terminators containing natural nucleobases *theoretically* lack the intrinsic selectivity to inhibit one DNA polymerase versus another.[2] Finally, since these agents resemble their natural counterparts, they may be degraded by cellular enzymes that metabolize natural nucleotides (*26*). For example, enzymatic deamination of purine analogues such as dideoxyadenosine limits its use (*27*) and may play a significant role in the development of drug resistance to natural nucleoside analogues.

To combat these complications, we attempted to exploit several of the unique features of the previously described nonnatural nucleotides that are displayed in Figure 1A (*28*, *29*, preceding manuscript). Specifically, we demonstrate that two of these nonnatural nucleotides are selectively inserted opposite damaged DNA that can be induced by chemotherapeutic agents. More importantly, these molecules act as potent and selective chain terminators of replication beyond an abasic site. This activity will inhibit the propagation of genomic errors caused by extending beyond a natural mispair. In general, the ability to selectively inhibit promutagenic DNA synthesis would be beneficial in preventing a leading culprit in disease development and drug resistance.

MATERIALS AND METHODS

Materials. [γ-^{32}P]ATP was purchased from M. P. Bio-Medicals. Ultrapure, unlabeled dNTPs were obtained from Pharmacia. Magnesium acetate and Trizma base were from Sigma. Urea, acrylamide, and bisacrylamide were from Aldrich. Oligonucleotides, including those containing a tetrahydrofuran moiety mimicking an abasic site, were synthesized by Operon Technologies (Alameda, CA). Single-stranded and duplex DNA were purified and quantified as described (*30*). All other materials were obtained from commercial sources and were of the highest available quality. The wild-type gp43 and the exonuclease-deficient mutant of gp43 (Asp-219 to Ala mutation) were purified and quantified as previously described (*31*, *32*). The nonnatural nucleotides used in this study were synthesized and purified as described (*29*, preceding manuscript).

Enzyme Assays. The assay buffer used in all kinetic studies consisted of 25 mM Tris-OAc (pH 7.5), 150 mM KOAc, and 10 mM 2-mercaptoethanol. All assays were performed at 25 °C. Polymerization reactions were monitored by analysis of the products on 20% sequencing gels as previously (*33*). Gel images were obtained with a Packard PhosphorImager using the OptiQuant software supplied by the manufacturer. Product formation was quantified by measuring the ratio of ^{32}P-labeled extended and nonextended primer. The ratios of product formation are corrected for substrate in the absence of polymerase (zero point). Corrected ratios are then multiplied by the concentration of primer/template used in each assay to yield total product. All concentrations are listed as final solution concentrations.

Competition Experiments. Ten nanomolar gp43 exo$^-$ was preincubated with 1000 nM 13/20-mer. To accurately visualize elongation, the 13-mer primer strand was labeled with [γ-^{32}P]ATP using T4 polynucleotide kinase (New England Biolabs) and annealed with a stoichiometric amount of unlabeled 20-mer. The polymerization reaction was initiated by the addition of 10 μM dNTPs (dATP, dGTP, dTTP) in the absence or presence of 500 μM 5-NITP. Five microliter aliquots of the reaction were quenched into tubes containing 5 μL of 200 mM EDTA at times ranging from 5 to 180 s. The quenched samples were processed as described above and product formation was analyzed using established protocols (*34*).

Competition assays during translesion DNA synthesis were performed with several slight modifications to the aforementioned protocol. First, single turnover conditions were employed in which 1000 nM gp43 exo$^-$ was preincubated with 250 nM 13/20SP-mer. As above, the 13-mer primer strand was labeled with [γ-^{32}P]ATP using T4 polynucleotide kinase and annealed with a stoichiometric quantity of unlabeled 20SP-mer. Second, the polymerization reaction was initiated by the addition of 500 μM dNTPs (dATP, dGTP, dTTP) in the absence and presence of 20 μM 5-NITP. Aliquots of the reaction were quenched into 200 mM EDTA at times ranging from 5 to 300 s and processed as described above.

Pre-Steady-State Exonuclease Assays. A rapid quench instrument was used to monitor the time course in hydrolysis of DNA containing a variety of mispaired primer−templates. In these experiments, a preincubated solution of 2 μM gp43 exo$^+$/10 mM Mg^{2+} was mixed with 500 nM 5′-labeled DNA (final concentrations). The reaction was then terminated at various times by the addition of 350 mM EDTA, and the reaction products were analyzed as described above. In all cases, the data were plotted as initial substrate (typically 14-mer) remaining as a function of time. Data for each time course were fit to eq 1 defining a first-order decay in initial substrate concentration.

$$y = A\,e^{-kt} + C \quad (1)$$

[2] A recent review by Lee et al. (*25*) points out that nucleoside analogues such as AZT and stavudine (d4T) used in the treatment of HIV infection differ in toxicity by 6 orders of magnitude despite possessing natural nucleobases. In these instances, the apparent selectivity observed in vivo correlates with the measured in vitro kinetics of nucleotide incorporation and excision. The influence of these activities on the potential toxic effects of our nonnatural nucleotide analogues is discussed more thoroughly within the Results and Discussion.

Scheme 1: Mechanism of Idle Turnover of dXTP Opposite an Abasic Site or Thymine[a]

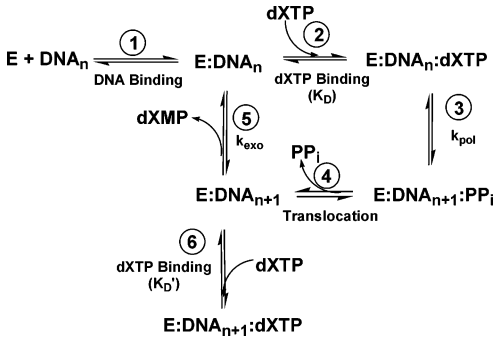

[a] Individual steps along the pathway are numbered and identified as follows: step 1 represents the binding of polymerase to DNA and is defined as the $K_{D\ DNA}$; step 2 represents the binding of dXTP to the polymerase/DNA complex and is defined as the $K_{D\ dXTP}$; step 3 represents the rate constant in DNA polymerization and is denoted as k_{pol}; step 4 represents translocation and pyrophosphate release; step 5 represents the rate constant of exonucleolytic degradation of DNA_{n+1} to yield DNA_n and is defined as k_{exo}; step 6 represents the binding of dXTP to the polymerase/DNA complex at the next templating position and is denoted as K_D'. Abbreviations are defined as follows: E = gp43 exo$^+$, DNA_n = DNA substrate, PP_i = inorganic pyrophosphate, and DNA_{n+1} = DNA product (DNA extended by one nucleobase).

where *A* is the burst amplitude, *k* is the observed rate constant for product formation, and *C* is the end point of the reaction.

Idle-Turnover Measurements. DNA (13/20SP-mer or 13/20T-mer; 250 nM) was first preincubated with variable concentrations of 5-NITP (20−200 μM) or 5-PhITP (10−200 μM) in the presence of 30 μM dATP. Due to the nature of the DNA substrate (Figure 1B), the insertion of dAMP opposite T at position 13 in the template maintains a usable primer template for the insertion of the nonnatural nucleotide opposite the abasic lesion (position 14). In all cases, the reaction was initiated through the addition of 1000 nM DNA gp43 exo$^+$. Five microliter aliquots of the reaction were quenched into tubes containing 5 μL of 200 mM EDTA at times ranging from 5 to 600 s. The quenched samples were processed as described above and product formation was analyzed using established protocols (*34*).

Simulations modeling the observed kinetic time courses for nucleotide insertion and excision were performed by mathematical analyses using KINSIM (*35*). A simplified mechanism depicted in Scheme 1 was employed that accounts for the kinetic parameters of interest. These minimally include K_D values for each nucleotide, k_{pol} values for their insertion, and k_{exo}, which represents the hydrolytic rate constant. Both the starting reactant concentrations and rate constants were supplied for each step of the mechanism. In all cases, the rate constants were based upon either experimentally determined rate constants or published literature values. The simulated curves were then compared to those experimentally derived to judge how accurately each set of rate constants fit the experimental data. Adjustments to the rate constants were then made until the simulated time courses were nearly identical to the experimental time courses.

RESULTS AND DISCUSSION

5-NITP and 5-PhITP Are Chain Terminators of DNA Synthesis. It was previously demonstrated that gp43 exo$^-$ can extend beyond an abasic site only when dAMP or dGMP are placed opposite the lesion (*36*). The ability to extend beyond these mispairs was proposed to reflect the positioning of these nucleobases in an interhelical position when paired opposite an abasic site (*36*). Since 5-NITP (*28*) and 5-PhITP (preceding manuscript) are more efficiently inserted opposite an abasic site, it was predicted that gp43 exo$^-$ would easily extend beyond these nonnatural analogues since they should exist in an interhelical conformation when paired opposite this lesion. This hypothesis was directly tested by measuring the ability of gp43 exo$^-$ to extend beyond either mispair using the experimental protocol outlined in Figure 2A. Briefly, the preincubated gp43 exo$^-$:13/20SP-mer complex was incubated with 50 μM dXTP for 30 s. This time frame allows all of the primer to be elongated by only one base, that is, conversion of 13-mer to 14-mer (Figure 2B, lane 2). After this time frame, 1000 μM dGTP was added to allow extension beyond the enzymatically formed 5-NIMP:abasic site mispair. Surprisingly, the polymerase cannot elongate beyond the 14-mer product even when supplied with high concentrations of the next correct dNTP. Increasing the reaction time, the concentration of dGTP, or both has no effect on extension (data not shown). The phenomenon is not limited to 5-NITP since identical results are obtained using 5-PhITP as the nucleotide substrate (data not shown).

Figure 2C displays the results from the positive control experiment monitoring incorporation and elongation beyond the DNA lesion when only natural dNTPs are used. As expected, gp43 exo$^-$ incorporates dATP opposite the abasic site. Extension beyond the formed dAMP:abasic site occurs when dGTP is added to the reaction mixture since a variety of polymerization products ranging from 15- to 17-mers accumulate. Thus, replication beyond an abasic site does occur, albeit with low efficiency.

The inability to extend beyond nonnatural nucleosides indicates that both 5-NITP and 5-PhITP are chain terminators of DNA synthesis. At face value, these results appear contradictory to our original hypothesis stating that the kinetics of elongation should be dependent upon the interhelical conformation of the nucleobase (*36*). However, alternative mechanisms distinct from perturbations in inter- versus extrahelical conformation could also account for the lack of extension. One possibility could reflect improper size or geometrical constraints imposed by the nonnatural mispair. For example, distortion of the newly formed mispair could cause the polymerase to stall or prevent translocation to the next templating position. Indeed, Hogg et al. (*37*) provide structural evidence for this mechanism using the RB69 DNA polymerase positioned at an abasic site. Their structural work indicates that the primer−template junction becomes distorted when dAMP is inserted opposite the lesion (*37*). Specifically, the formed mispair and several adjacent base pairs are tilted and twisted in such a way that the polymerase is unable to translocate to the next correct templating position. This structural information coincides well with the poor kinetics of elongation and could easily explain the lack of elongation beyond these mispairs. Another potential mechanism invokes the contributions of various heterocyclic nitrogens during the polymerization cycle. In this regard, several groups have demonstrated that purine analogues devoid of either the N7 or N3 nitrogens are effectively inserted into DNA but are refractory to elongation (*38*−*41*).

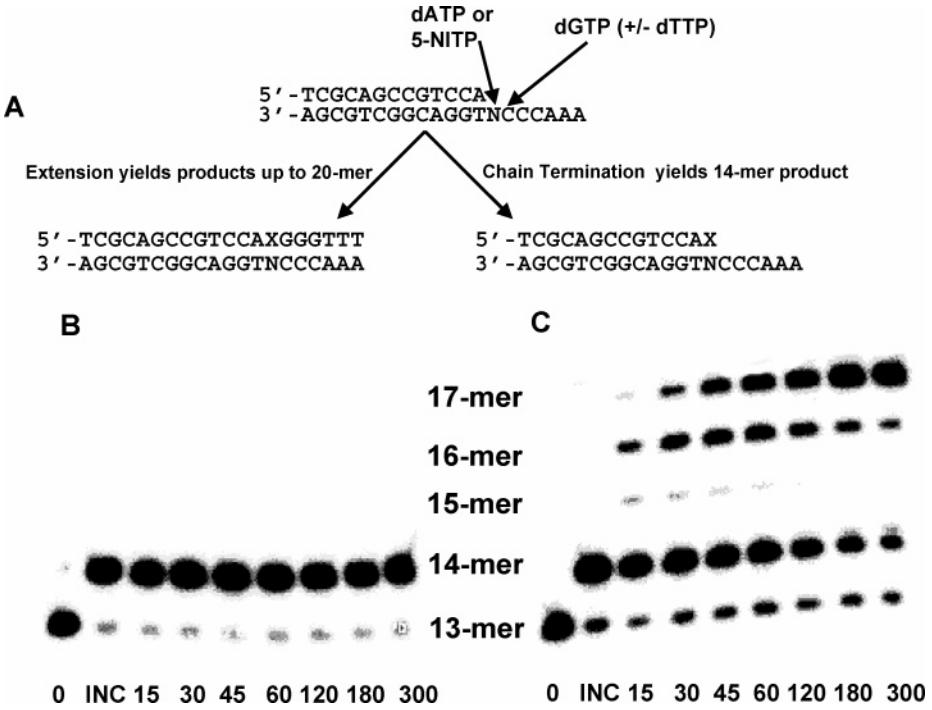

FIGURE 2: 5-NITP is a chain terminator of translesion DNA synthesis. (A) Protocol used to measure the ability of gp43 exo$^-$ to extend beyond nonnatural mispairs. Assays monitoring translesion DNA synthesis were performed mixing a preincubated solution of 1 μM gp43 exo$^-$, 500 nM 5′-labeled 13/20SP-mer, and 10 mM Mg^{2+} with 50 μM 5-NITP for 30 s (B) or 500 μM dATP for 3 min (C). In both cases, 1000 μM dGTP was then added to allow for elongation beyond the formed mispair. The reaction was then terminated at various times by the addition of 200 mM EDTA at time intervals ranging from 5 to 300 s. Nucleotide incorporation was analyzed by denaturing gel electrophoresis.

These results again demonstrate that typical hydrogen-bonding functional groups are not necessary for incorporation. However, their presence appears obligatory for efficient elongation. In fact, these functional groups are proposed to be required for minor groove contacts between the nucleic acid and DNA polymerase (*39*). It is easy to envision that the removal of these contacts could prevent translocation of the polymerase, disturb the orientation of the primer/template, or both to inhibit elongation.

Potency and Selectivity for Inhibiting Replication Beyond an Abasic Site. The previous data indicate that replication beyond an abasic site could be selectively inhibited by 5-NITP and 5-PhITP. The next goal was to determine whether these nonnatural nucleotides could effectively compete with natural dNTPs for insertion opposite an abasic site under in vivo relevant conditions. This was accomplished using an adaptation of the protocol illustrated in Figure 2A using unmodified DNA or DNA containing an abasic site (Figure 1B). This experimental paradigm has two distinct advantages. The first is that it directly measures the ability of 5-NITP (or 5-PhITP) to compete with natural dNTPs for insertion opposite damaged or unmodified DNA (potency and selectivity). Second, it measures the ability of these nonnatural analogues to prevent elongation beyond potential mispairs and evaluates the potential efficacy of these compounds.

As a positive control, the ability of gp43 exo$^-$ to insert and elongate beyond the abasic site was measured in the absence of either 5-NITP or 5-PhITP. Since replication beyond this form of DNA damage is typically disfavored (*36*), high concentrations of natural dNTPs (500 μM each) were used to enhance insertion and extension beyond this form of DNA damage. In the absence of any nonnatural nucleotide, gp43 exo$^-$ inserts and extends beyond the abasic site fairly efficiently (Figure 3A).[3] The slow rate constant of 0.18 ± 0.02 s^{-1} measured for the elongation of the 13-mer recapitulates previously published data (*36*).

Figure 3B however shows the results of a competition experiment performed in the presence of 20 μM 5-NITP and 500 μM dNTPs. Denaturing gel electrophoresis shows that there is a rapid production of 14-mer that reflects the exclusive incorporation of 5-NITP opposite the abasic site. A more important observation, however, is that the level of 14-mer product remains invariant during the time course of the reaction. Identical results are obtained when the experiment is performed substituting 5-PhITP for 5-NITP (data not shown). The inability of gp43 exo$^-$ to extend beyond the generated mispairs provides a clear indication of the chain termination abilities of 5-NITP and 5-PhITP. Furthermore, this inhibition is not observed when the reaction is performed using IndTP, 5-FITP, or 5-AITP at a fixed concentration of 20 μM (data not shown). Increasing the concentration of these analogues to 350 μM has no effect on the kinetics of elongation (data not shown). The inability of these analogues to inhibit replication beyond an abasic site likely arises from the fact that all three analogues have high K_D and low k_{pol} values for insertion opposite the abasic site (preceding paper).

The potency of 5-NITP toward inhibiting replication beyond an abasic site was further quantified by measuring the dose dependence of 5-NITP toward inhibiting primer elongation. Experiments were performed as described above

[3] dAMP is presumably inserted opposite the lesion under these conditions since the measured K_d and k_{pol} values for dATP incorporation are significantly more favorable than those for other natural dNTPs (*36*).

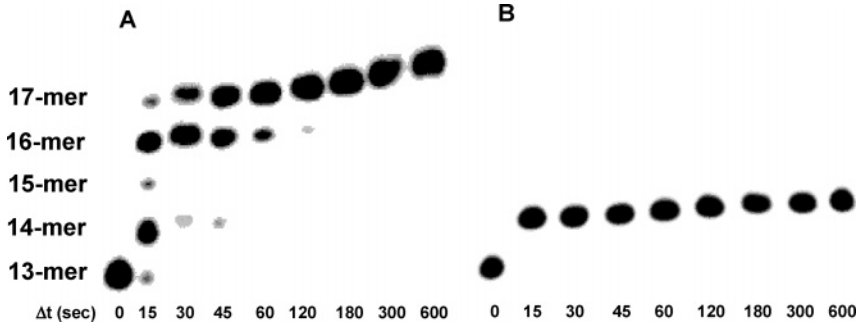

FIGURE 3: 5-NITP competes with dATP for binding to the DNA polymerase during translesion DNA synthesis. The gp43 exo$^-$ (1 μM) and 5′-labeled 13/20SP-mer (250 nM) were preincubated in the presence of 10 mM Mg^{2+} and mixed with 500 μM dATP and 1000 μM dGTP in the absence (A) or presence of 20 μM NITP (B). In both cases, the reactions were terminated at various times by the addition of 200 mM EDTA at time intervals ranging from 5 to 600 s. Nucleotide incorporation was analyzed by denaturing gel electrophoresis.

with the exception that the concentration of 5-NITP was varied at 0, 5, 10, and 20 μM (Supporting Information). As expected, extension beyond the abasic site occurs in the absence of nonnatural nucleotide. However, the amount of extension decreases as the concentration of 5-NITP is increased. The IC_{50} value for 5-NITP is 10 μM since this concentration inhibits 50% of primer extension. Similar analyses for 5-PhITP yield an IC_{50} value of 10 μM (data not shown). Collectively, these data indicate that 5-NITP and 5-PhITP can effectively compete with natural dNTPs for the binding to the polymerase and can inhibit translesion DNA synthesis.

Chain Termination Capabilities Using Unmodified DNA. The ability of these nonnatural nucleotides to function as generic chain terminators was also evaluated using an unmodified DNA substrate. In these experiments, pseudo-first-order conditions were used since normal DNA synthesis is more efficient than translesion DNA synthesis. Specifically, a limiting concentration of gp43 exo$^-$ (10 nM) was preincubated with 1000 nM 13/20-mer prior to the addition of 10 μM dNTPs in the absence (Figure 4A) or in the presence of 500 μM 5-NITP (Figure 4B). In the absence of 5-NITP, a ladder of products ranging from 14-mers to 20-mers is observed, a result that demonstrates the ability of the polymerase to easily elongate unmodified DNA. The wide distribution of elongation products reflects the low processivity of the polymerase under pseudo-first-order conditions (*42*). Visual inspection of the data provided in Figure 4B reveals that the addition of 500 μM 5-NITP has little effect on the ability of gp43 exo$^-$ to perform normal DNA synthesis. Further quantification of the reaction products indicates that the addition of 500 μM 5-NITP reduces the overall rate in primer elongation by less than 10% (Figure 4C). The slight degree of inhibition on the rate and extent of primer elongation indicates that 5-NITP has low potency for terminating synthesis on undamaged DNA. Nearly identical results are obtained when 5-PhITP is substituted for 5-NITP (data not shown). The ability of other nonnatural nucleotides to inhibit normal DNA synthesis was also evaluated. High concentrations (500 μM) of other nonnatural nucleosides such as IndTP, 5-FITP, or 5-AITP do not inhibit normal DNA synthesis (data not shown). As before, the inability to inhibit normal DNA synthesis likely reflects their poor kinetic parameters for insertion opposite natural templating bases, that is, high K_D and low k_{pol} values (preceding paper).

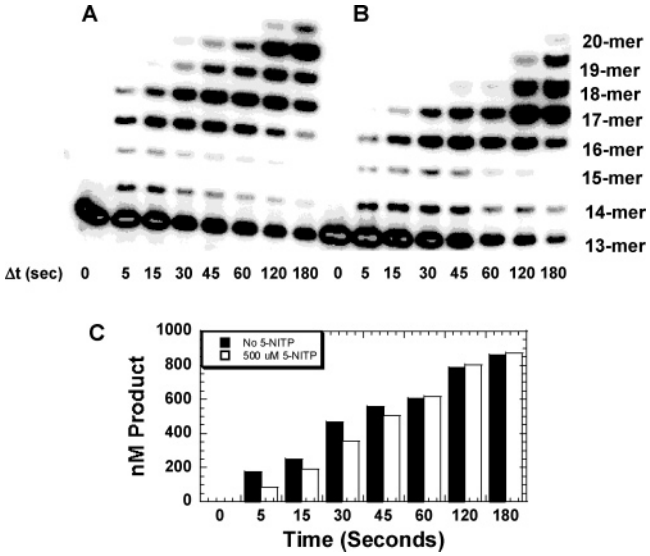

FIGURE 4: 5-NITP does not inhibit DNA synthesis using undamaged DNA. Ten nanomolar gp43 exo$^-$ and 1000 nM 5′-labeled 13/20-mer were preincubated in the presence of 10 mM Mg^{2+} and mixed with 10 μM dNTPs (dATP, dGTP, and dTTP) in the absence (A) or presence of 500 μM NITP (B). In both cases, the reactions were terminated at various times by the addition of 200 mM EDTA at time intervals ranging from 5 to 300 s. Nucleotide incorporation was analyzed by denaturing gel electrophoresis. Panel C reports the amount of product formed as a function of time.

Stability of 5-NITP Incorporation Opposite Natural or Damaged DNA. The associated exonuclease activity of the DNA polymerase can effectively remove most chain terminators from DNA after being incorporated. In the case of our nonnatural nucleotides, this activity would render the analogue therapeutically useless. To address this concern, we evaluated the ability of gp43 exo$^+$ to excise 5-NIMP from DNA when it is placed opposite the nontemplating lesion or opposite T. The advantage of the bacteriophage T4 enzyme is that it possesses a vigorous exonuclease activity that plays a significant role in the maintenance of fidelity (*30*). Excision reactions were performed employing single turnover conditions in a rapid quench instrument. The first set of experiments compare the excision of 5-NIMP and dAMP when paired opposite an abasic site (Figure 5). Time courses in excision are best defined as a single-exponential curve. An observed rate constant of excision (k_{exo}) of 9.9 $\pm$ 0.8 s^{-1} is measured for excising 5-NIMP, while the k_{exo} value for excising dAMP is 28.5 $\pm$ 1.1 s^{-1}.

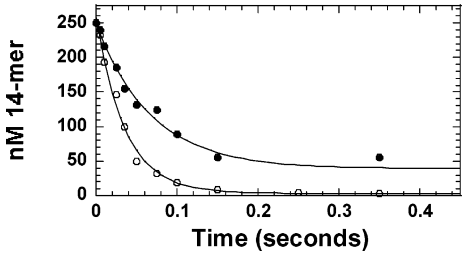

FIGURE 5: 5-NIMP is excised more slowly than dAMP when placed opposite an abasic site. The time course in excision of dXMP opposite the lesion was performed mixing a preincubated solution of 1 μM gp43 exo$^+$/10 mM Mg^{2+} with 250 nM 5′-labeled DNA/10 mM Mg^{2+} (final concentrations) and terminating the reaction at various times by the addition of 350 mM EDTA. The time course in dAMP excision is represented by filled circles, while that for 5-NIMP excision is represented by open circles. Each time course represents an average of three independent determinations. Time courses were fit to the equation for single-exponential decay, $y = A\ e^{-kt} + C$, where A is the burst amplitude, k is the observed rate constant for product formation, and C is the end point of the reaction. The rate constant, k_{exo}, for excising dAMP is 28.5 ± 1.1 s^{-1}, while that for measured for 5-NIMP excision is 9.9 ± 0.8 s^{-1}.

Table 1: Summary of Exonuclease Rate Constants Measured for the Excision of dAMP or 5-NIMP Paired Opposite an Abasic Site or Thymine[a]

primer nucleoside	template nucleoside	k_{exo} (s^{-1})
dAMP	thymine	0.8 ± 0.1
dAMP	abasic site	28.5 ± 1.1
5-NITP	thymine	13.0 ± 1.4
5-NITP	abasic site	9.9 ± 0.8

[a] The kinetic rate constant, k_{exo}, was measured under single turnover reaction conditions using 1 μM gp43 exo$^+$, 250 nM DNA (14A/20T-mer, 14A/20SP-mer, 14NI/20T-mer, or 14NI/20SP-mer), and 10 mM Mg^{2+}.

Surprisingly, the kinetics of 5-NIMP excision placed opposite T are nearly identical to that measured for excision opposite the abasic site (Supporting Information) as reflected in the k_{exo} value of 13.0 ± 1.4 s^{-1}, which is nearly identical to that measured for excision opposite the abasic site. Control experiments measuring the excision of dAMP when paired opposite T reveal that excision of dAMP is significantly slower since the k_{exo} value is 0.8 ± 0.1 s^{-1}. This value is consistent with the published value of 2 s^{-1} (*30*).

Comparing the rate constants of excision summarized in Table 1 provides interesting insights into the dynamics of exonuclease proofreading. First, the rate constant for dAMP excision opposite the abasic site is ~40-fold faster than that measured when the natural nucleotide is paired opposite T. The faster rate constant undoubtedly reflects the nature of the mispair. Not surprisingly, the rate constant for excising 5-NIMP from an abasic site is 3-fold slower than that for dAMP excision from the same lesion. We argue that this difference reflects the increased base-stacking capabilities of 5-NIMP compared to dAMP (*37*) such that the increased stability of the 5-NIMP:abasic site makes it more difficult to partition the primer into the exonuclease active site for degradation. This argument is consistent with biochemical (*43*) and structural (*37*, *44*) data indicating that at least three base pairs have to be melted for the primer to partition to the exonuclease active site of the bacteriophage polymerase.

This model may also explain the similarity in rate constants for excising 5-NIMP from T versus an abasic site. This result was surprising since it was predicted that the 5-NIMP:T mispair would be hydrolyzed much faster than the 5-NIMP:SP mispair.[4] This prediction is based upon the generally accepted kinetic model for fidelity in which the rates of dNMP excision (k_{exo}) are inversely correlated with the rates of dNTP incorporation (k_{pol}). The basis for this model is intuitively obvious: the more difficult it is to form a mispair, the easier it should be to degrade it and vice versa. We have demonstrated that this correlation exists during translesion DNA synthesis with natural nucleotides since it is kinetically unfavorable to incorporate dATP opposite an abasic site ($k_{pol} \approx 0.15$ s^{-1}) while it is kinetically favorable to excise dAMP ($k_{exo} \approx 28$ s^{-1}). Although the majority of data with natural mispairs support this argument (*45*−*47*), the dynamics of exonuclease proofreading may be different when nonnatural nucleotides are placed in the primer. For example, we previously demonstrated that the incorporation of 5-NITP opposite an abasic site ($k_{pol} = 126$ s^{-1}) is kinetically favored by 140-fold compared to the insertion of 5-NITP opposite T ($k_{pol} = 0.9$ s^{-1}) (*28*). The kinetic difference arguably reflects the enhanced stability of the 5-nitro-indole opposite the abasic site rather than when paired opposite T in the template. Since the 5-NIMP:T mispair appears less favorable, it stands to reason that it should be rapidly degraded. However, the k_{exo} value of ~10 s^{-1} for excision from opposite T is essentially identical to that measured for excision from the "favored" mispair of 5-NIMP:SP. It is tempting to speculate that the identity in kinetics for excision of 5-NIMP from different mispairs reflects the universal base-stacking properties of the nonnatural nucleobase (*48*). Current efforts are underway to evaluate this mechanism.

Idle Turnover Measurements. Idle turnover is a process in which the DNA polymerase incorporates a dNTP and then excises the inserted dNMP in the absence of the next required nucleotide triphosphate (Scheme 1). This activity provides a more accurate representation of in vivo conditions in which the polymerase should be bound and stalled at the sight of DNA damage. Idle turnover was quantified using a modified gel electrophoresis protocol that monitors the amount of extension (13-mer to 14-mer) and subsequent excision (14-mer to 13-mer) of the DNA as a function of time. All experiments were performed using single turnover reaction conditions to ensure that all DNA was bound with polymerase during the course of the reaction. Under these conditions, the rates in product formation reflect the kinetics of insertion and excision rather than enzyme dissociation from the mispair. In each experiment, the concentration of nonnatural nucleotide was varied from 20 to 200 μM. In addition, a low concentration of 30 μM dATP was used to allow for correct dNMP insertion at position 13-mer, which prevents complete degradation of DNA substrate.[5]

[4] The identity in excision rate constants could reflect intrinsic difficulties in processing the nonnatural nucleobase. This mechanism appears unlikely since the kinetics for degrading single-stranded DNA containing 5-NIMP are identical to that for the degradation of unmodified single-stranded DNA (data not shown).

[5] Incorporation of dATP opposite T (position 13 in the template) maintains a usable primer for the insertion of the nonnatural nucleotide opposite the abasic lesion (position 14). dAMP insertion opposite the abasic site presumably does not occur since the concentration of dATP was maintained subsaturating at 30 μM.

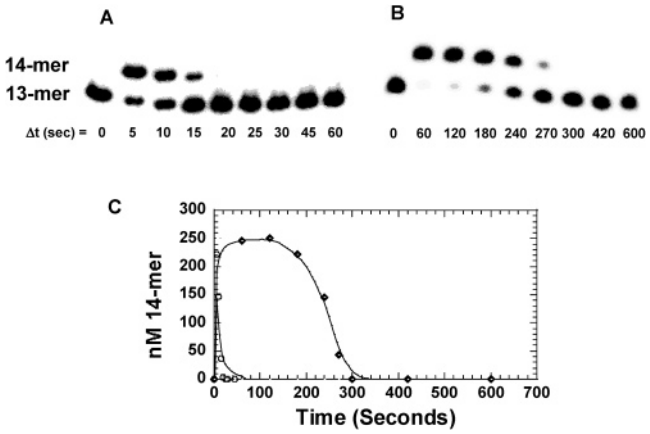

FIGURE 6: Representative gel electrophoresis data for the idle turnover of 5-NITP during insertion opposite an abasic site. One micromolar gp43 exo$^+$ was added last to a solution containing 250 nM 5′-labeled 13/20SP-mer, 10 mM Mg^{2+}, and 20 μM NITP (A) or 200 μM NITP (B). Reactions were terminated by the addition of 200 mM EDTA at time intervals ranging from 5 to 600 s. Nucleotide incorporation and excision were analyzed by denaturing gel electrophoresis. Panel C reports the amount of product formed as a function of time using 5-NITP concentrations of 20 (○) and 200 μM (◆), respectively.

Figure 6A shows representative denaturing gel electrophoresis data for the idle turnover of 5-NITP opposite the abasic site at 20 and 200 μM 5-NITP, respectively. Figure 6B provides the time courses monitoring the production of 14-mer under these conditions and reveals that the accumulation of 14-mer is both concentration- and time-dependent. At either concentration, there is rapid primer elongation to form 14-mer since the catalytic efficiency for 5-NITP incorporation opposite the lesion is high ($k_{pol}/K_D = 7.0 \times 10^6$ M^{-1} s^{-1}) (*25*, *33*). The steady-state accumulation of 14-mer product reflects the latency in degradation that defines the process of idle turnover. It is clear, however, that there is an attenuation in the time course for 14-mer degradation as the concentration of 5-NITP is increased from 20 to 200 μM. This dose dependency can easily be explained by the law of mass action since the concentration of nucleotide substrate diminishes during this steady-state phase due to repetitive cycling of insertion and excision. Under these conditions, the concentration of 5-NITP decreases until it is below the K_D value. At this point, the polymerase is unable to continue incorporation opposite the lesion, and this leads to complete degradation of the 14-mer.

To validate this model, computer simulations of the data were performed using the mechanism provided in Scheme 1. Since single turnover reaction conditions were employed, kinetic steps reflecting enzyme dissociation and rebinding to product DNA are assumed to be negligible. Thus, the rate and amount of 14-mer produced are dependent upon four interrelated parameters. These include the kinetic dissociation constant (K_D) for dXTP opposite the lesion (DNA_n) (step 2), the rate constant for DNA extension (k_{pol}) (step 3), the rate constant of exonuclease degradation (k_{exo}) (step 5), and the kinetic dissociation constant (K_D') for dXTP opposite the next templating position (DNA_{n+1}) (step 6). Although k_{pol} is a complex function of kinetic rate constants, this value was simplified to combine the kinetic steps encompassing the conformational change prior to phosphoryl transfer, phosphoryl transfer, and the conformational change after phosphoryl transfer. Furthermore, translocation of the enzyme and pyrophosphate release (step 4) are assumed to be rapid.

Initial computer simulations were performed using the published K_D value of 18 μM and the k_{pol} value of 126 s^{-1} for 5-NITP incorporation opposite an abasic site (*28*). The experimentally measured value of 10 s^{-1} was used for k_{exo} (vide supra). At a fixed concentration of 5-NITP (20 μM), the time course in the production and subsequent degradation of 14-mer could only be adequately fit if a parameter that represented the kinetic equilibrium dissociation constant (K_D') for 5-NITP opposite the next templating position (DNA_{n+1}) was included in the simulations. Computer simulations were also performed for the time courses generated at several different fixed concentrations of 5-NITP (20, 50, 100, and 200 μM). In all cases, time courses were best fit using the following parameters: K_D value of 20 μM, a k_{pol} value of 100 s^{-1}, a k_{exo} value of 10 s^{-1}, and a K_D' value of 10 mM.

Identical analyses were performed to measure the idle turnover of 5-PhITP as the nucleotide substrate. The data provided in Figure 7 compares the time courses generated for the incorporation of 100 μM 5-PhITP versus 100 μM 5-NITP opposite the abasic site. It is clear that the phenyl-indole derivative is more stably incorporated opposite the abasic site compared to the nitro indole analogue. This result is somewhat surprising since the overall catalytic efficiency for 5-PhITP incorporation opposite the lesion ($k_{pol}/K_D = 3.6 \times 10^6$ M^{-1} s^{-1}) is 2-fold lower than that measured for 5-NITP ($k_{pol}/K_D = 7.0 \times 10^6$ M^{-1} s^{-1}). Regardless, the enhanced stability of 5-PhIMP opposite the lesion is indicative of a decrease in idle turnover. This reduction could be caused at two mutually exclusive mechanisms that would be reflected in perturbations in two different kinetic steps along the reaction pathway. The first step would be a reduced rate constant in degradation (k_{exo}), while the alternative is a reduction in the K_D' value for the next templating position. Computer simulation was again used to generate values corresponding to K_D, k_{pol}, k_{exo}, and K_D' (Table 2). The parameter most sensitive to variation is the k_{exo} value. In fact, this value is 10-fold slower than that measured for the excision of 5-NIMP from opposite the abasic site. This result indicates that it is more difficult to excise the large phenyl-indole derivative than the smaller 5-nitro analogue. It is tempting to speculate that the reduced rate constant in exonuclease degradation reflects the enhanced base-stacking capabilities of the 5-phenyl-indole derivative.

Potential Toxicity and Therapeutic Indices of the Non-Natural Nucleotides. These results collectively indicate that nonnatural nucleotides 5-NITP and 5-PhITP can effectively inhibit replication beyond an abasic site under in vitro conditions. To place constraints on the potential in vivo utility of these analogues to inhibit promutagenic versus normal DNA replication, we employed the methodologies outlined by Lee et al. (*25*) to define the potential toxicity and therapeutic indices of 5-NITP and 5-PhITP. It should be noted that we define potential toxicity as the inhibition of replication beyond an abasic site. While the term "toxic" is used as a descriptor, this activity is considered to be beneficial since it would potential prevent promutagenic DNA synthesis. Briefly, the potential effectiveness of each

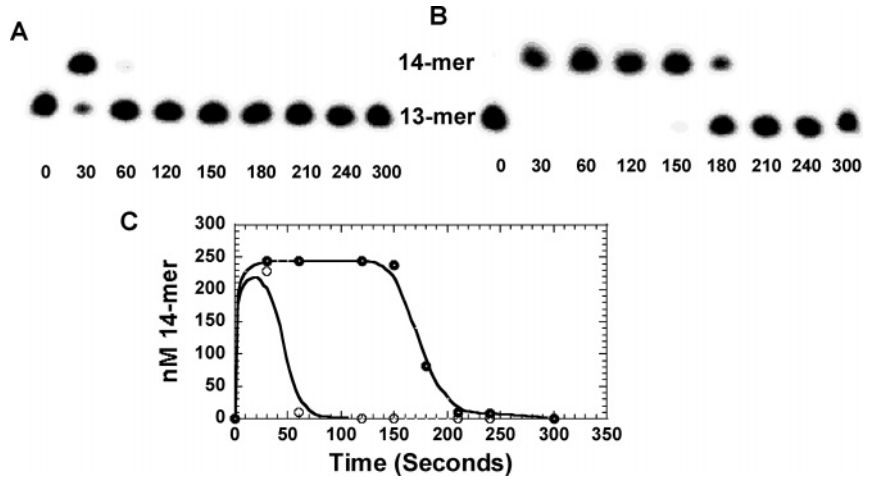

FIGURE 7: Comparison of idle turnover kinetics for 5-NITP and 5-PhITP insertion opposite an abasic site. One micromolar gp43 exo$^+$ was added last to a solution containing 250 nM 5′-labeled 13/20SP-mer, 10 mM Mg^{2+}, and 100 μM 5-NITP (A) or 100 μM 5-PhITP (B). Reactions were terminated by the addition of 200 mM EDTA at time intervals ranging from 30 to 300 s. Nucleotide incorporation and excision were analyzed by denaturing gel electrophoresis. Panel C reports the amount of product formed as a function of time using 100 μM 5-NITP (○) or 100 μM 5-PhITP (●), respectively.

Table 2: Summary of Kinetic Rate and Equilibrium Constants Measured for the Idle Turnover of 5-Nitro-indolyl-2′-deoxyriboside Triphosphate (5-NITP) and 5-Phenyl-indolyl-2′-deoxyriboside Triphosphate (5-PhITP) Opposite an Abasic Site

dXTP	K_D (μM)	k_{pol} (s^{-1})	k_{exo} (s^{-1})	K_D' (μM)
5-NITP	20 ± 5	100 ± 10	10 ± 2	$10\,000 \pm 1000$
5-PhITP	20 ± 5	50 ± 10	1.0 ± 0.1	$10\,000 \pm 1000$

analogue to inhibit replication beyond an abasic site was evaluated by measuring the catalytic efficiency, k_{pol}/K_D, for both analogues and then calculating the discrimination for insertion as the ratio of catalytic efficiencies for the nucleotide analogue versus the correct dNTP. Among the four natural nucleotides, dATP has the highest k_{pol}/K_D value for incorporation opposite an abasic site and is therefore considered to be the correct dNTP for replication opposite this lesion. In the case of incorporation opposite an abasic site, discrimination (*D*) is defined as $(k_{pol}/K_D)_{dATP}/(k_{pol}/K_D)_{dXTP}$. Using 5-NITP as the nonnatural nucleotide, we can calculate the discrimination factor as 7×10^6 M^{-1} s^{-1}/4300 M^{-1} s^{-1} yielding a value for *D* of 6.1×10^{-4} (Table 3). Similar analyses were used to calculate a *D* value of 11.4×10^{-5} for 5-PhITP (Table 3). Both values are extremely low and provide a clear indication that the nonnatural nucleotides should be exclusively incorporated opposite an abasic site. We note that this conclusion is true *only* if the concentrations of dATP and dXTP are equal. It is obvious that these discrimination values will approach unity if the concentration of dATP increases in relationship to that of the nonnatural nucleotide, a condition that may occur within an in vivo context due to potential differences in absorption and metabolism.

Regardless, these favorable discrimination values predict that 5-NITP and 5-PhITP have the potential to be chemopreventive agents. As previously noted, however, the associated exonuclease activity of the DNA polymerase could effectively remove them to render these analogues therapeutically useless. As such, the combined contributions of incorporation and excision must be considered when evaluating the potential therapeutic utility of any nucleotide analogue. This can be evaluated by calculating the toxicity

Table 3: Summary of Calculated Discrimination Values, Toxicity Index, and Therapeutic Index for 5-Nitro-indolyl-2′-deoxyriboside Triphosphate (5-NITP) and 5-Phenyl-indolyl-2′-deoxyriboside Triphosphate (5-PhITP)

parameter	5-NITP	5-PhITP
discrimination (abasic DNA)[a]	6.1×10^{-4}	11.4×10^{-4}
discrimination (unmodified DNA)[a]	53	460−2500
toxicity index (abasic DNA)[b]	6	33
toxicity index (unmodified DNA)[b]	0.047	0.01−0.05
therapeutic index[c]	128	660−3300

[a] Discrimination (*D*) is defined as $(k_{pol}/K_D)_{dXTP}/(k_{pol}/K_D)_{dATP}$. [b] The toxicity index for each analogue was calculated as $(k_{pol\ dNTP}/k_{exo\ dXTP})$(dXTP/dNTP)/(4*D*) where $k_{pol\ dNTP}$ represents the maximal rate of polymerization of the natural dNTP, $k_{exo\ dXTP}$ represents the maximal rate of excision of the nonnatural nucleotide, (dXTP/dNTP) is the ratio of nonnucleotide and natural nucleotide concentrations, and *D* is the discrimination factor (*25*). [c] The therapeutic index of each nonnatural nucleotide was calculated using the toxicity index for abasic containing DNA divided by the toxicity index using normal DNA.

index, which is defined as $(k_{pol\ dNTP}/k_{exo\ dXTP})$(dXTP/dNTP)/(4*D*) where $k_{pol\ dNTP}$ represents the maximal rate of polymerization of the natural dNTP, $k_{exo\ dXTP}$ represents the maximal rate of excision of the nonnatural nucleotide, (dXTP/dNTP) is the ratio of nonnucleotide and natural nucleotide concentrations, and *D* is the aforementioned calculated discrimination factor (*25*). This value defines the relative increase in time that would be required to extend beyond an abasic site based upon the rate constants for incorporation and excision of the nonnatural nucleotide. In the case of 5-NITP, this value is ~6, while that for 5-PhITP is ~33 (Table 3). The difference in values reflects the slower excision of 5-PhIMP compared to 5-NIMP and suggests that 5-PhITP would be more effective toward inhibiting replication opposite an abasic site.

We next evaluated the potential of 5-NITP and 5-PhITP to provide what we consider to be a true toxic response by inhibiting normal DNA synthesis, i.e., stable incorporation opposite unmodified DNA. As outlined above, discrimination

can be calculated by the ratio of $(k_{pol}/K_D)_{dXTP}/(k_{pol}/K_D)_{dNTP}$ for incorporation opposite templating nucleobase. In the case of unmodified DNA, we find that the *D* value for 5-NITP is ~53, while that for 5-PhITP is 460−2500.[6] These extremely high values indicate that nonnatural nucleotide, especially 5-PhITP, should be rarely incorporated opposite any of the four natural nucleobases. Furthermore, these values can be used to calculate the toxicity index of 0.047 for 5-NITP and 0.01−0.05 for 5-PhITP (Table 3). The importance of these low values is that neither analogue should give a toxic response by inhibiting normal DNA synthesis since they are not stably incorporated opposite unmodified DNA.

Finally, the therapeutic index of each nonnatural nucleotide was calculated using the toxicity indices for the inhibition of normal DNA synthesis and replication beyond an abasic site. The therapeutic index (TI) of a drug defines how selective it may be toward producing a desired effect rather than an adverse one and is classically defined as the ratio of the toxic dose (TD) in relation to its effective dose (ED) (*49*). In computing this value, we designate that the toxic dose reflects inhibition of replication on unmodified DNA, while the effective dose reflects inhibition of replication beyond an abasic site, or the toxicity index for abasic containing DNA/the toxicity index using normal DNA. Calculating the TI for 5-NITP, we find that this value is ~128. The calculated value for 5-PhITP is 660−3300 and is more favorable than that calculated for 5-NITP. The importance of these values is that the difference suggests that 5-PhITP would be "safer" than 5-NITP as a chemopreventive agent. However, this conclusion needs to be validated through careful in vivo analyses.

Conclusions. This report outlines the development of a series of novel nonnatural nucleotide analogues that act as selective inhibitors of replication opposite an abasic site. We demonstrate that two analogues containing substituent groups with extended conjugated systems (5-NITP and 5-PhITP) are preferentially incorporated opposite an abasic site. Furthermore, the potency and efficacy of these analogues is reflected in their high affinity for incorporation opposite the lesion ($K_D \approx 10\ \mu$M) and their ability to terminate DNA synthesis with low IC_{50} values of ~10 μM. Finally, these molecules were more resistant to enzymatic excision when placed opposite an abasic site compared to natural nucleotides such as dATP.

These results have several important ramifications toward the development and implementation of these analogues as innovative chemotherapeutic agents. Since these nonnatural nucleotides are selectively inserted opposite abasic sites, they may potentiate the cytotoxic effects of DNA damaging agents such as temozolomide and cyclophosphamide that can increase the formation of abasic sites by enhancing the spontaneous rate of depurination (*50*) or through DNA repair mechanisms (*51*). Our nucleotide analogues could potentiate the cytotoxic effects of these chemotherapeutic agents since they may inhibit the repair of lesions caused by various DNA damaging compounds. The benefit of potentiation is that lower doses of DNA damaging agents could be administered to reduce the potential for common side effects including immunosuppression, nausea, and allopecia that are associated with these agents (*52*).

An additional advantage of these nonnatural nucleotides lies in their chemopreventive potential when used in combination with DNA damaging chemotherapeutic agents. This aspect is important since a significant concern of chemotherapy is the generation of mutational errors caused by the inappropriate replication of unrepaired DNA lesions caused by DNA damaging agents. Indeed, it is now recognized that the development of secondary cancers can arise from inadvertent mutagenesis caused by chemotherapeutic drugs that induce DNA damage (*53*). One prevalent example is treatment-related acute myeloid leukemia (tAML), which can develop after exposure to DNA alkylating agents such as chlorambucil and cyclophosphamide (*54*, *55*). These nonnatural nucleotides could be instrumental in the prevention of secondary cancers since they would inhibit the propagation of genomic errors caused by DNA damaging agents. We note that the calculated toxicity and therapeutic indices are lower than what would be expected for a truly effective and potent chain terminator (*25*). However, these low values arise from the rigorous exonuclease proofreading associated with the bacteriophage T4 polymerase. We hypothesize that these values will be higher depending upon the DNA polymerase. For example, error prone DNA polymerase such as pol η (*56*) and pol κ (*57*) are devoid of or have significantly reduced exonuclease activity. A reduction or omission in exonuclease activity coupled with high discrimination in insertion would significantly increase the toxicity index of these nonnatural nucleotides. Since error-prone DNA polymerases are proposed to be responsible for replicating beyond most DNA lesions (*58*), including abasic sites (*59*), we speculate that the toxicity index for nonnatural nucleotides such as 5-PhITP will be considerably higher than that reported here once tested for in vivo efficacy.

SUPPORTING INFORMATION AVAILABLE

Time courses monitoring the excision of 5-NIMP and dAMP when paired opposite an abasic site as well as the excision of 5-NIMP and dAMP when paired opposite T. This material is available free of charge via the Internet at http://pubs.acs.org.

REFERENCES

1. Massague, J. (2004) G1 cell-cycle control and cancer. *Nature 432*, 298−306.
2. Eguchi, K. (2001) Apoptosis in autoimmune diseases. *Intern. Med. 40*, 275−284.
3. Sharma, P. L., Nurpeisov, V., Hernandez-Santiago, B., Beltran, T., and Schinazi, R. F. (2004) Nucleoside inhibitors of human immunodeficiency virus type 1 reverse transcriptase. *Curr. Top. Med. Chem. 4*, 895−919.
4. Rogers, B. L. (2004) Bacterial targets to antimicrobial leads and development candidates. *Curr. Opin. Drug Discovery Dev. 7*, 11−22.
5. Danson, S. J., and Middleton, M. R. (2001) Temozolomide: a novel oral alkylating agent. *Expert. Rev. Anticancer Ther. 1*, 13−19.
6. Ludeman, S. M. (1999) The chemistry of the metabolites of cyclophosphamide. *Curr. Pharm. Des. 5*, 627−643.
7. Fuertesa, M. A., Castillab, J., Alonsoa, C., and Perez, J. M. (2003) Cisplatin biochemical mechanism of action: from cytotoxicity to

[6] Variations in the toxicity index are calculated for 5-PhITP since the measured catalytic efficiency for its incorporation opposite templating nucleobases varies from 4.0×10^3 to 21.7×10^3 $M^{-1}sec^{-1}$ (preceding manuscript).

induction of cell death through interconnections between apoptotic and necrotic pathways. *Curr. Med. Chem. 10*, 257−266.
8. Bradbury, P. A., and Middleton, M. R. (2004) DNA repair pathways in drug resistance in melanoma. *Anticancer Drugs 15*, 421−426.
9. Janatova, M., Zikan, M., Dundr, P., Matous, B., and Pohlreich, P. (2005) Novel somatic mutations in the BRCA1 gene in sporadic breast tumors. *Hum. Mutat. 25*, 319.
10. Kishimoto, M., Kohno, T., Okudela, K., Otsuka, A., Sasaki, H., Tanabe, C., Sakiyama, T., Hirama, C., Kitabayashi, I., Minna, J. D., Takenoshita, S., and Yokota J. (2005) Mutations and deletions of the CBP gene in human lung cancer. *Clin. Cancer Res. 11*, 512−519.
11. Linja, M. J., and Visakorpi, T. (2004) Alterations of androgen receptor in prostate cancer. *J. Steroid Biochem. Mol. Biol. 92*, 255−264.
12. Griesinger, F., Metz, M., Trumper, L., Schulz, T., and Haase, D. (2004) Secondary leukaemia after cure for locally advanced NSCLC: alkylating type secondary leukaemia after induction therapy with docetaxel and carboplatin for NSCLC IIIB. *Lung Cancer 44*, 261−265.
13. Karran, P., Offman, J., and Bignami, M. (2003) Human mismatch repair, drug-induced DNA damage, and secondary cancer. *Biochimie 85*, 11459−11460.
14. Chaudhary, U. B., and Haldas, J. R. (2003) Long-term complications of chemotherapy for germ cell tumours. *Drugs 63*, 1565−1577.
15. Papadopulos-Eleopulos, E., Turner, V. F., Papadimitriou, J. M., Causer, D., Alphonso, H., and Miller, T. (1999) A critical analysis of the pharmacology of AZT and its use in AIDS. *Curr. Med. Res. Opin.* (Suppl 1), S1−45.
16. Elion, G. B. (1993) Acyclovir: discovery, mechanism of action, and selectivity. *J. Med. Virol.* (Suppl 1), 2−6.
17. Villahermosa, M. L., Martinez-Irujo, J. J., Cabodevilla, F., and Santiago, E. (1997) Synergistic inhibition of HIV-1 reverse transcriptase by combinations of chain-terminating nucleotides. *Biochemistry 36*, 13223−13231.
18. Fraley, A. W., Chen, D., Johnson, K., and McLaughlin, L. W. (2003) An HIV reverse transcriptase-selective nucleoside chain terminator. *J. Am. Chem. Soc. 125*, 616−617.
19. Reardon, J. E. (1989) Herpes simplex virus type 1 and human DNA polymerase interactions with 2′-deoxyguanosine 5′-triphosphate analogues. Kinetics of incorporation into DNA and induction of inhibition. *J. Biol. Chem. 264*, 19039−19044.
20. Matsuda, A., and Sasaki, T. (2004) Antitumor activity of sugar-modified cytosine nucleosides. *Cancer Sci. 95*, 105−111.
21. Arion, D., and Parniak, M. A. (1999) HIV resistance to zidovudine: the role of pyrophosphorolysis. *Drug Resist. Updates 2*, 91−95.
22. Reha-Krantz, L. J. (1998) Regulation of DNA polymerase exonucleolytic proofreading activity: studies of bacteriophage T4 "antimutator" DNA polymerases. *Genetics 148*, 1551−1557.
23. Cardoen, S., Van Den Neste, E., Smal, C., Rosier, J. F., Delacauw, A., Ferrant, A., Van den Berghe, G., and Bontemps, F. (2001) Resistance to 2-chloro-2′-deoxyadenosine of the human B-cell leukemia cell line EHEB. *Clin. Cancer Res. 7*, 3559−3566.
24. Dumontet, C., Bauchu, E. C., Fabianowska, K., Lepoivre, M., Wyczechowska, D., Bodin, F., and Rolland, M. O. (1999) Common resistance mechanisms to nucleoside analogues in variants of the human erythroleukemic line K562. *Adv. Exp. Med. Biol. 457*, 571−577.
25. Lee, H., Hanes, J., and Johnson, K. A. (2003) Toxicity of nucleoside analogues used to treat AIDS and the selectivity of the mitochondrial DNA polymerase. *Biochemistry 42*, 14711−14719.
26. Simhadri, S., Kramata, P., Zajc, B., Sayer, J. M., Jerina, D. M., Hinkle, D. C., and Wei, C. S. (2002) Benzo[*a*]pyrene diol epoxide-deoxyguanosine adducts are accurately bypassed by yeast DNA polymerase zeta *in vitro*. *Mutat. Res. 508*, 137−145.
27. Zhang, Y., Wu, X., Guo, D., Rechkoblit, O., Taylor, J. S., Geacintov, N. E., and Wang, Z. (2002) Lesion bypass activities of human DNA polymerase mu. *J. Biol. Chem. 277*, 44582−44587.
28. Reineks, E. Z., and Berdis, A. J. (2004) Evaluating the contribution of base stacking during translesion DNA replication. *Biochemistry 43*, 393−404.
29. Zhang, X., Lee, I., and Berdis, A. J. (2004) Evaluating the contributions of desolvation and base-stacking during translesion DNA synthesis. *Org. Biomol. Chem. 2*, 1703−1711.
30. Capson, T. L., Peliska, J. A., Kaboord, B. F., Frey, M. W., Lively, C., Dahlberg, M., and Benkovic, S. J. (1992) Kinetic characterization of the polymerase and exonuclease activities of the gene 43 protein of bacteriophage T4. *Biochemistry 31*, 10984−10994.
31. Frey, M. W., Nossal, N. G., Capson, T. L., and Benkovic, S. J. (1993) Construction and characterization of a bacteriophage T4 DNA polymerase deficient in 3′→5′ exonuclease activity. *Proc. Natl. Acad. Sci. U.S.A. 90*, 2579−2583.
32. Rush, J., and Konigsberg, W. H. (1989) Rapid purification of overexpressed T4 DNA polymerase. *Prepr. Biochem. 19*, 329−340.
33. Mizrahi, V., Benkovic, P. A., and Benkovic, S. J. (1986) Mechanism of DNA polymerase I: exonuclease/polymerase activity switch and DNA sequence dependence of pyrophosphorolysis and misincorporation reactions. *Proc. Natl. Acad. Sci. U.S.A. 83*, 5769−5773.
34. Berdis, A. J. (2003) Analysis of translesion DNA replication using transient kinetic methodologies. *Recent Research Developments in Analytical Biochemistry*, Transworld Research Network.
35. Barshop, B. A., Wren, R. F., and Frieden, C. (1983) Analysis of numerical methods for computer simulation of kinetic processes: development of KINSIM- -a flexible, portable system. *Anal. Biochem. 130*, 134−145.
36. Berdis, A. J. (2001) Dynamics of translesion DNA synthesis catalyzed by the bacteriophage T4 exonuclease-deficient DNA polymerase. *Biochemistry 40*, 7180−7191.
37. Hogg, M., Wallace, S. S., and Doublie, S. (2004) Crystallographic snapshots of a replicative DNA polymerase encountering an abasic site. *EMBO J. 23*, 1483−1493.
38. Switzer, C. Y., Moroney, S. E., and Benner, S. A. (1993) Enzymatic recognition of the base pair between isocytidine and isoguanosine. *Biochemistry 32*, 10489−10496.
39. Morales, J. C., and Kool, E. T. (2000) Functional hydrogen-bonding map of the minor groove binding tracks of six DNA polymerases. *Biochemistry 39*, 12979−12988.
40. Mitsui, T., Kitamura, A., Kimoto, M., To, T., Sato, A., Hirao, I., and Yokoyama, S. (2003) An unnatural hydrophobic base pair with shape complementarity between pyrrole-2-carbaldehyde and 9-methylimidazo[(4,5)-*b*]pyridine. *J. Am. Chem. Soc. 125*, 5298−5307.
41. Matsuda, S., Henry, A. A., Schultz, P. G., and Romesberg, F. E. (2003) The effect of minor-groove hydrogen-bond acceptors and donors on the stability and replication of four unnatural base pairs. *J. Am. Chem. Soc. 125*, 6134−6139.
42. Mace, D. C., and Alberts, B. M. (1984) T4 DNA polymerase. Rates and processivity on single-stranded DNA templates. *J. Mol. Biol. 177*, 295−311.
43. Cowart, M., Gibson, K. J., Allen, D. J., and Benkovic, S. J. (1989) DNA substrate structural requirements for the exonuclease and polymerase activities of procaryotic and phage DNA polymerases. *Biochemistry 28*, 1975−1983.
44. Wang, J., Sattar, A. K., Wang, C. C., Karam, J. D., Konigsberg, W. H., and Steitz, T. A. (1997) Crystal structure of a pol alpha family replication DNA polymerase from bacteriophage RB69. *Cell 89*, 1087−1099.
45. Donlin, M. J., Patel, S. S., and Johnson, K. A. (1991) Kinetic partitioning between the exonuclease and polymerase sites in DNA error correction. *Biochemistry 30*, 538−546.
46. Beechem, J. M., Otto, M. R., Bloom, L. B., Eritja, R., Reha-Krantz, L. J., and Goodman, M. F. (1998) Exonuclease-polymerase active site partitioning of primer-template DNA strands and equilibrium Mg^{2+} binding properties of bacteriophage T4 DNA polymerase. *Biochemistry 37*, 10144−10155.
47. Jin, Y. H., Garg, P., Stith, C. M., Al-Refai, H., Sterling, J. F., Murray, L. J., Kunkel, T. A., Resnick, M. A., Burgers, P. M., and Gordenin, D. A. (2005) The multiple biological roles of the 3′→5′ exonuclease of *Saccharomyces cerevisiae* DNA polymerase delta require switching between the polymerase and exonuclease domains. *Mol. Cell. Biol. 25*, 461−471.
48. Smith, C. L., Simmonds, A. C., Felix, I. R., Hamilton, A. L., Kumar, S., Nampali, S., Loakes, D., and Brown, D. M. (1998) DNA polymerase incorporation of universal base triphosphates. *Nucleosides Nucleotides 17*, 541−554.

49. Sausville, E. A. (2004) Optimizing target selection and development strategy in cancer treatment: the next wave. *Curr. Med. Chem. Anti-Cancer Agents 4*, 445−447.
50. Lindahl, T. (1990) Repair of intrinsic DNA lesions. *Mutat. Res. 238*, 305−311.
51. Allinson, S. L., Sleeth, K. M., Matthewman, G. E., and Dianov, G. L. (2004) Orchestration of base excision repair by controllingthe rates of enzymatic activities. *DNA Repair (Amsterdam) 3*, 23−31.
52. van Vollenhoven, R. F. (2004) Benefits and risks of biological agents: lymphomas. *Clin. Exp. Rheumatol. 22*, S122−S125.
53. Grunwald, H. W., and Rosner, F. (1998) Secondary acute leukemia in chronic lymphocytic leukemia. *N. Engl. J. Med. 339*, 924.
54. Smith, R. E. (2003) Risk for the development of treatment-related acute myelocytic leukemia and myelodysplastic syndrome among patients with breast cancer: review of the literature and the National Surgical Adjuvant Breast and Bowel Project experience. *Clin. Breast Cancer 4*, 273−279.
55. Karp, J. E., and Smith, M. A. (1997) The molecular pathogenesis of treatment-induced (secondary) leukemias: foundations for treatment and prevention. *Semin. Oncol. 24*, 103−113.
56. Matsuda, T., Bebenek, K., Masutani, C., Hanaoka, F., and Kunkel, T. A. (2000) Low fidelity DNA synthesis by human DNA polymerase-eta. *Nature 404*, 1011−1013.
57. Friedberg, E. C. (2001) Why do cells have multiple error-prone DNA polymerases? *Environ. Mol. Mutagen. 38*, 105−110.
58. Faili, A., Aoufouchi, S., Weller, S., Vuillier, F., Stary, A., Sarasin, A., Reynaud, C. A., and Weill, J. C. (2004) DNA polymerase eta is involved in hypermutation occurring during immunoglobulin class switch recombination. *J. Exp. Med. 199*, 265−270.
59. Ohashi, E., Ogi, T., Kusumoto, R., Iwai, S., Masutani, C., Hanaoka, F., and Ohmori H. (2000) Error-prone bypass of certain DNA lesions by the human DNA polymerase kappa. *Genes Dev. 14*, 1589−1594.

BI050584N